Eur Biophys J (2007) 36:779–786
DOI 10.1007/s00249-007-0172-0

ORIGINAL PAPER

Ca^{2+} current of frog vestibular hair cells is modulated by intracellular ATP but not by long-lasting depolarisation

Marta Martini · Federica Farinelli · Maria Lisa Rossi · Giorgio Rispoli

Received: 29 December 2006 / Revised: 18 April 2007 / Accepted: 24 April 2007 / Published online: 22 May 2007
© EBSA 2007

Abstract Some aspects of Ca^{2+} channel modulation in hair cells isolated from semicircular canals of the frog (*Rana esculenta*) have been investigated using the whole-cell technique and intra and extracellular solutions designed to modify the basic properties of the Ca^{2+} macrocurrent. With 1 mM ATP in the pipette solution, about 60% of the recorded cells displayed a Ca^{2+} current constituted by a mix of an L and a drug-resistant (R2) component; the remaining 40% exhibited an additional drug-resistant fraction (R1), which inactivated in a Ca-dependent manner. If the pipette ATP was raised to 10 mM, cells exhibiting the R1 current fraction displayed an increase of both the R1 and L components by ~280 and ~70%, respectively, while cells initially lacking R1 showed a similar increase in the L component with R1 becoming apparent and raising up to a mean amplitude of ~44 pA. In both cell types the R2 current fraction was negligibly affect by ATP. The current run-up was unaffected by cyclic nucleotides, and was not triggered by 10 mM ATPγS, ADP, AMP or GTP. Long-lasting depolarisations (>5 s) produced a progressive, reversible decay in the inward current despite the presence of intracellular ATP. Ca^{2+} channel blockade by Cd^{2+} unmasked a slowly activating outward Cs^{+} current flowing through a non-Ca^{2+} channel type, which became progressively unblocked by prolonged depolarisation even though Cs^{+} and TEA^{+} were present on both sides of the channel. The outward current waveform could be erroneously ascribed to a Ca- and/or voltage dependence of the Ca^{2+} macrocurrent.

Proceedings of the XVIII Congress of the Italian Society of Pure and Applied Biophysics (SIBPA), Palermo, Sicily, September 2006.

M. Martini · F. Farinelli · M. L. Rossi · G. Rispoli (✉)
Dipartimento di Biologia ed Evoluzione,
Sezione di Fisiologia e Biofisica, e Centro di Neuroscienze,
Università di Ferrara, Via L. Borsari, 46, 44100 Ferrara, Italy
e-mail: rsg@unife.it

Keywords Frog semicircular canals · Hair cells · Patch-clamp · Voltage-gated Ca^{2+} channels · Ca^{2+} channel modulation · ATP

Introduction

Ca^{2+} inflow through basolateral, voltage-gated Ca^{2+} channels of vestibular hair cells plays a crucial role in signal processing because it sustains transmitter release at the cytoneural junction and regulates membrane excitability (Rossi et al. 1994; Martini et al. 2000; Fuchs 2002; Lelli et al. 2003).

Three distinct Ca^{2+} channel types have been identified in frog canal hair cells according to their biophysical and pharmacological properties (Martini et al. 2000). The one carrying most of the current is a non-inactivating L-type channel that has also been found in many other hair cell types (Su et al. 1995; Green et al. 1996; Kollmar et al. 1997; Martini et al. 2000; Platzer et al. 2000; Rodriguez-Contreras and Yamoah 2001; Rodriguez-Contreras et al. 2002; Bao et al. 2003; Brandt et al. 2003); in particular, in turtle auditory hair cells, the entire Ca^{2+} current appears to flow through this channel type (Schnee and Ricci 2003). The two other channels have been tentatively identified as R-type on the basis of their resistance to dihydropyridines, ω-cono- and aga-toxins. The first channel, termed R1, shows Ca^{2+}-dependent inactivation; the second, R2, sustains a non-inactivating current. Although evidence for a non-L Ca^{2+} current has been provided for many other hair cell types (Su et al. 1995; Lopez et al. 1999; Rodriguez-Contreras and Yamoah 2001; Rodriguez-Contreras et al. 2002; Brandt et al. 2003; Waka et al. 2003), molecular biology analysis has yet to demonstrate conclusively the presence of R-type channel proteins in semicircular canal

hair cells. Therefore "R1" and "R2" tags should be considered mainly a phenomenological, operatively useful notation.

The L and R2 currents, which activate at −60 mV and peak at −20 mV, may sustain the ongoing spontaneous transmitter release at the cytoneural junction, whereas the R1 component, which activates at a more positive membrane potential and peaks at −30 mV, may be functionally important in evoking the fast synchronous transmitter release in response to short, strong stimuli (Martini et al. 2000). Any mechanism controlling the size of these currents would thus strongly affect transmitter release at the cytoneural junction and consequently the flow of sensory information towards the CNS. In particular, it has been found that Ca^{2+} channels are regulated either via a G protein—(reviewed in Dolphin 2003) or via a phosphorylation pathway (reviewed in Catterall 2000). Likewise the mode of channel activation was similarly relevant: prolonged depolarisation (>1 s) actually resulted in a long-term inactivation of the Ca^{2+} current in turtle auditory hair cell (Schnee and Ricci 2003) and in other preparations (Hering et al. 2004). In the present work, some possible factors of Ca^{2+} channel regulation—namely, ATP-related intracellular effects and time-dependent membrane depolarisation—have been investigated in vestibular hair cells of the frog semicircular canal. It is shown that R1 and L currents are boosted by ATP, but at difference from turtle auditory hair cells, long-lasting depolarising steps did not markedly inactivate the Ca^{2+} current. A preliminary report of this work has been presented (Martini et al. 2006).

Materials and methods

Cell preparation and solutions

The experiments were performed on frogs (*Rana esculenta*, 25–40 g body weight) as previously described (Martini et al. 2000; Rispoli et al. 2000, 2001). Animals were handled in compliance with the Declaration of Helsinki guidelines. Briefly, frogs were anaesthetised by immersion in a tricaine methane sulphonate solution (1 g/l in water) and then decapitated. The six ampullae were isolated from both labyrinths and transferred into a dissection chamber (500 µl volume). The hair cells were mechanically dissociated from the ampullae by gently scraping the epithelium with fine forceps (dissection solution composition was, in mM: 120 NaCl, 2.5 KCl, 0.5 EGTA, 5 HEPES, 20 sucrose, 3 glucose; pH ≈ 7.2, osmolality ≈ 260 mOsmol/kg).

The extracellular solution composition was (mM): 100 NaCl, 6 CsCl, 20 TEACl, 4 $CaCl_2$ (or 4 $BaCl_2$), 10 HEPES, 6 Glucose (pH 7.2, 260 mOsmol/kg). The Ca^{2+} current was reduced by adding 10 µM nifedipine (dissolved in dimethyl sulfoxide) to the external solution or blocked by the addition of 200 µM Cd^{2+}. K^+ channel blockers such as 0.5–2 µM apamin, 0.5–1 µM charybdotoxin, and 200 nM iberiotoxin were also tested. Solutions containing Ba^{2+} and/or these channel blockers were perfused on the cell in rapid (∼50 ms) succession. This was achieved by using a computer-controlled stepping motor to horizontally move a multibarrelled perfusion pipette, aligned in front of the recorded cell. The hair cells in the recording chamber were continuously perfused with the extracellular solution fed in by a peristaltic pump (Masterflex, Cole-Parmer, Vernon, IL, USA) that also removed the solutions applied via the perfusion pipette.

The intracellular solution composition was (mM): 90 CsCl, 20 TEACl, 2 $MgCl_2$, 1 adenosine 5′-triphosphate K^+ salt (ATP), 0.1 guanosine 5′-triphosphate Na^+ salt (GTP), 10 HEPES, 5 EGTA (pH 7.2, 235 mOsm/kg). In some experiments, ATP was raised to 10 mM or, alternatively, 10 mM adenosine 5′-[γ-thio]triphosphate tetra Li^+ salt (ATPγS), 10 mM adenosine 5′-diphosphate Na^+ salt (ADP), 10 mM adenosine 5′-monophosphate Na^+ salt (AMP) were added to the standard solution. The effect of cyclic nucleotides was tested by adding 1 mM guanosine 3′,5′-cyclic monophosphate Na^+ salt (cGMP) or 1 mM adenosine 3′,5′-cyclic monophosphate Na^+ salt (cAMP) to the ATP-containing intracellular solution. In low Cs^+ experiments, some or all of the pipette Cs^+ was substituted with an isoosmolar amount of *N*-methyl-glucamine (NMG^+). Reagents were purchased from Sigma Chemical Co. (St Louis, MO, USA), Alomone Labs (Israel) and Merck-Calbiochem (Darmstadt, Germany).

Patch-clamp recording and data analysis

Whole-cell Ca^{2+} current was recorded at room temperature (20–22°C) using an EPC-7 amplifier (List-Electronic, Darmstadt, Germany). Cells were viewed on a TV monitor (Sony, Tokyo, Japan), connected to a contrast-enhanced video camera (T.I.L.L. Photonics, Planegg, Germany) coupled to an inverted microscope (Olympus IMT-2, Tokyo, Japan) equipped with Hoffman modulation contrast optics. Data were acquired using a Digidata 1322A computer interface and pClamp 9.0 software (Axon Instruments, Union City, CA, USA) running on a Pentium computer. The recordings were filtered at 10 kHz via an eight-pole Butterworth filter (LPBS-48DG, NPI Electronic, Tamm, Germany) and acquired at 40 kHz. The figures were prepared using a commercial plotting program (Version 8.0, Sigmaplot, Jandel Scientific, San Rafael, CA, USA). Data are presented as mean ± SEM.

Results and discussion

Nucleotide modulation of Ca^{2+} currents

In the presence of 1 mM ATP in the pipette solution approximately 60% of the hair cells, recorded in whole-cell mode, exhibited a steady Ca^{2+} current whose amplitude was maximal at −20 mV. The remaining cells (40%) were characterised by an initial current peak, followed by an exponential decay (inactivation) to a plateau level. Peak amplitude was maximal at −30 mV and inactivation was Ca^{2+}-dependent (Martini et al. 2000).

It was previously observed that upon repeating the depolarising step Ca^{2+} current amplitude could transiently increase before the run-down took place. This behaviour—reported for many other cellular systems and commonly referred to as current "run-up"—has occasionally been observed also in vestibular hair cells (Martini et al. 2000). In many cases, the run-up is sustained by a cyclic nucleotide-dependent or independent phosphorylation (reviewed in Catterall 2000). The former regulatory pathway was excluded in our preparation, since addition of 1 mM cGMP or 1 mM cAMP to the pipette solution did not run up the Ca^{2+} current at all. However, if ATP was raised to 10 mM, a robust run-up became manifest in all cells recorded: as intracellular ATP equilibrated with that of the pipette, the amplitude of both the inactivating current peak and the plateau component progressively increased by about 280 ± 74 and 70 ± 28%, respectively (n = 10; Fig. 1a). Cells initially lacking inactivation exhibited a similar plateau increase (63 ± 22%, n = 7) while the amplitude of the peak, initially absent, rose up to ~89 pA (44 ± 9 pA, n = 7; Fig. 1b). This increase was entirely sustained by the Ca^{2+} current run-up, since it was completely blocked by extracellular 200 μM Cd^{2+} (data not shown). Once the maximal run-up was achieved, inactivation was completely lost if the external Ca^{2+} was substituted with Ba^{2+} (Fig. 2), showing that the run-up of the inactivating component was entirely due to the rise in the R1 fraction. Finally, 10 μM nifedipine always reduced the plateau amplitude by the same amount, irrespective of the size attained when run-up was complete (Fig. 2). This indicates that high ATP did not activate any Ca^{2+} channel type other than those described above; rather it would appear that the ATP induced effect targeted the L and R1 components.

The cumulative addition of 1 mM cGMP or 1 mM cAMP to the 10 mM ATP internal solution did not cause any further increase in current, once more ruling out any modulation of the Ca^{2+} current via cyclic nucleotide-dependent phosphorylation. This ATP-dependent effect could be due to a direct nucleotide action on the channel (as first demonstrated for some L-type Ca^{2+} channels by Noma and Shibasaki 1985; Leresche et al. 2004). The possible binding

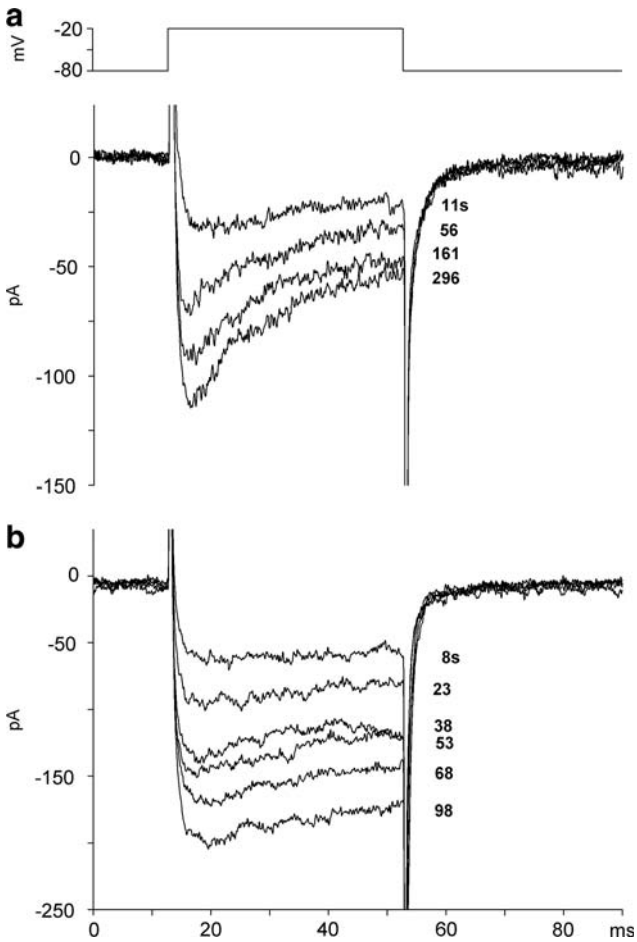

Fig. 1 Ca^{2+} current run-up induced by 10 mM ATP in response to successive 40 ms depolarisations from −80 to −20 mV, repeated every 15 s. Representative traces are shown at selected recording times (indicated close to each trace; breakthrough to whole-cell at zero time) for two different cells in which the inactivating R1 component was initially present (**a**) or absent (**b**)

of an adenosine residue to a specific channel site was ruled out, since no current run-up was manifest in the presence, in the pipette solution, of 10 mM AMP or 10 mM ADP alone.

Therefore, either an ATP-specific regulatory site actually exists, or modulation takes place by means of channel phosphorylation mediated by a specific kinase, as found in many other preparations (reviewed in Catterall 2000). Since no run-up was observed in the presence of 10 mM ATPγS (the non-hydrolysable analog of ATP), it can be suggested that the Ca^{2+} channel is regulated via a cyclic nucleotide-independent phosphorylation. Modulation required high nucleotide concentrations, since the run-up was less evident in the presence of 5 mM ATP (current run-down was, however, delayed vs. that observed in the presence of 1 mM ATP).

Moreover, increasing the Mg^{2+} concentration to 10 mM—in order to match the ATP concentration—did not boost the run-up process but rather reduced its extent.

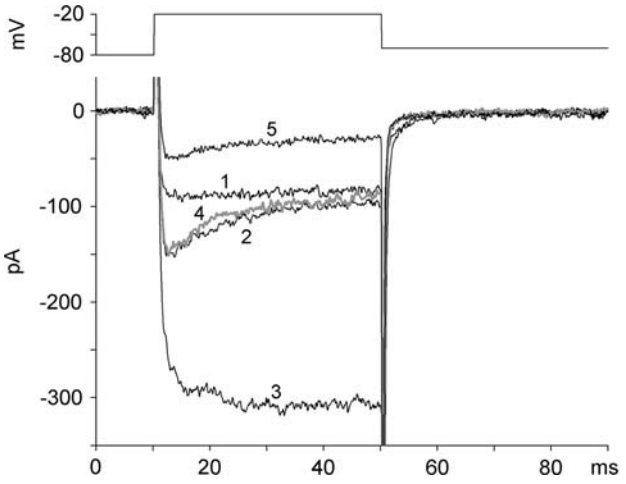

Fig. 2 Effect of Ba^{2+} and nifedipine applied during run-up. At the peak of current increase (*2*), 119 s after the breakthrough to whole-cell (*1*), the cell was exposed to a solution in which 4 mM Ca^{2+} was replaced by an isoosmolar concentration of Ba^{2+} (*3*). The *grey* trace (*4*) shows recovery after Ba^{2+} perfusion and then the cell was exposed to 10 μM nifedipine (*5*). For the sake of clarity, full recovery following nifedipine application was omitted

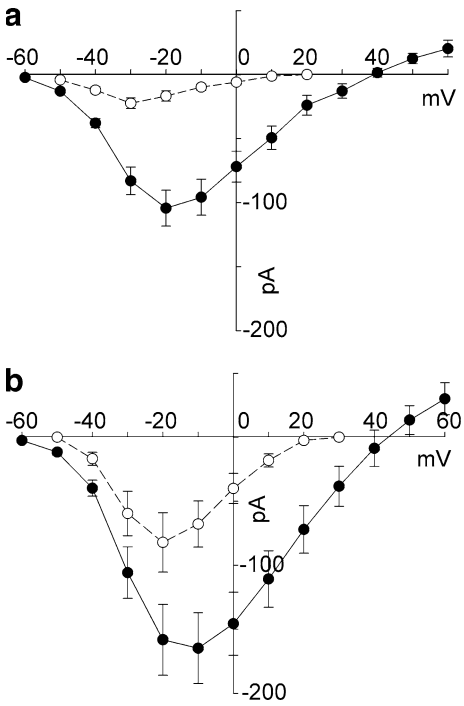

Fig. 3 Effect of ATP on the current to voltage relationships (I–Vs). *Empty* and *filled circles* refer to the average peak and plateau I–Vs, respectively, in 1 mM ATP (**a**) and 10 mM ATP (**b**). For each panel, maximal peak current, maximal plateau current and number of cells averaged were, respectively: −22 ± 4 pA, −104 ± 14 pA, $n = 10$ (**a**); −82 ± 23 pA, −165 ± 28 pA, $n = 10$ (**b**)

Many reports indicate that, in general, modulatory pathways targeted to ion channels affect their current-to-voltage relationship (I–V) and tail currents, although it has been found that ATP regulation of L-type Ca^{2+} channels is mainly the result of an increase in channel availability (as originally found by O'Rourke et al. 1992; Yazawa et al. 1997). On the other hand, extracellular ATP strongly affects the voltage dependence of cochlear outer hair cells, modifying both the I–V and tail currents (Chen et al. 1995). In order to precisely assess a possible intracellular ATP modulation of the voltage sensitivity of vestibular hair cells Ca^{2+} channels, the average I–Vs of the peak component (generated by the R1 channels) and of the plateau component (generated by the R2 and L channels; Martini et al. 2000) recorded in the presence of 1 mM (Fig. 3a) or 10 mM ATP (Fig. 3b) have been compared. No significant differences between the I–V profiles (peak and plateau) in 1 or 10 mM ATP were found out. A few cells (3/14) exhibiting run-up in 1 mM ATP were analysed separately: the shape of their I-Vs, however, was undistinguishable from controls. In all these tracings, the amplitude of the bi-exponential tail currents and their time constants upon returning to the holding potential (−70 mV) from any depolarisation level (reflecting the closure of L and R2 channels), were not affected by the ATP concentration and/or the run-up extent (for instance, the tail current for a depolarisation to −20 mV had always average time constants of ∼0.25 and ∼8 ms).

In hair cells, G-protein-mediated and phosphorylation pathways may coexist. The G-protein pathways are usually turned on by a ligand-activated membrane receptor, which has never been detected in vestibular hair cells. Nevertheless, it is possible to unmask the presence of a background G-protein regulation by increasing the GTP level from 0.1 mM (the concentration usually present) to 10 mM. This manoeuvre did not actually modify the size of the Ca^{2+} current: it can therefore be concluded that, if a G-protein pathway exists, it is silent in the absence of the specific activatory ligand.

The physiological role of Ca^{2+} channel modulation by ATP is most likely multifaceted and has yet to be fully elucidated. Among other things, it might be a safety mechanism to control intracellular Ca^{2+} levels in view of changes in ATP concentration. Indeed, substantial shifts in ATP concentration would modify the rate at which Ca^{2+} is removed by the Ca^{2+} ATP-ase pumps, thus leading to erratic Ca^{2+} changes (and transmitter release rates). Therefore ATP modulation of Ca^{2+} influx could compensate an ATP-induced change in Ca^{2+} efflux, making the afferent information less dependent on the intracellular ATP level. This perspective also concerns the resting activity of the hair cell cytoneural junction, where the internal Ca^{2+} concentration is likely to be permanently larger, and highly regulated, than in any other synaptic terminal to sustain the typical high-rate ongoing quantal release (Rossi et al. 1994).

Time-dependent modulation of Ca^{2+} current

Very long depolarisations (>5 s) produced a progressive current decay to a steady-state level despite the presence of intracellular ATP: the larger the depolarisation, the faster the decay, no matter what the current size (Fig. 4), internal ATP concentration (1 or 10 mM), and presence or absence of the R1 component. Initial current amplitude was fully recovered upon keeping the cell at the holding potential for >500 ms.

It has been suggested that this decay was a long-term effect induced on the Ca^{2+} current by depolarisation itself (Schnee and Ricci 2003), as found in other preparations (Hering et al. 2004). However, the steady level was usually outward for voltage steps exceeding 0 mV, indicating that the decay was not due to a simple Ca and/or voltage-dependent inactivation. In any case, since the input resistance did not change throughout the depolarising command, the current decay was not associated with progressive development of a leakage conductance (Figs. 6, 7). This large current decay was not present when the internal Cs^+ was substituted with NMG^+, and the current never became outward for any depolarisation amplitude (Fig. 5).

This demonstrates that the decay was actually generated by the progressive activation of an outward current carried by Cs^+, summating to (and even cancelling) the inward Ca^{2+} flow. Cs^+ movements, however, were not mediated by Ca-dependent K^+ channels of the SK (Tucker and Fettiplace 1996) or BK type, since the external application of 2 μM apamin, or 1 μM charybdotoxin, or 200 nM iberiotoxin and 20 mM TEA (occasionally 65 mM) present on both sides of the channel, did not affect the size of the outward current. Alternatively, Cs^+ outflow might occur through the Ca^{2+} channel itself: this would imply a progressive, voltage-dependent increase in channel permeability toward monovalent cations.

This possibility was, however, ruled out by testing Ca^{2+} versus Na^+ permeability after switching the external solution from 4 mM to 100 nM Ca^{2+}. This concentration was just enough to block the Ca^{2+} channel or to allow only a minor Na^+ influx through it. If there were a permeability change during long-lasting depolarisation, a progressively

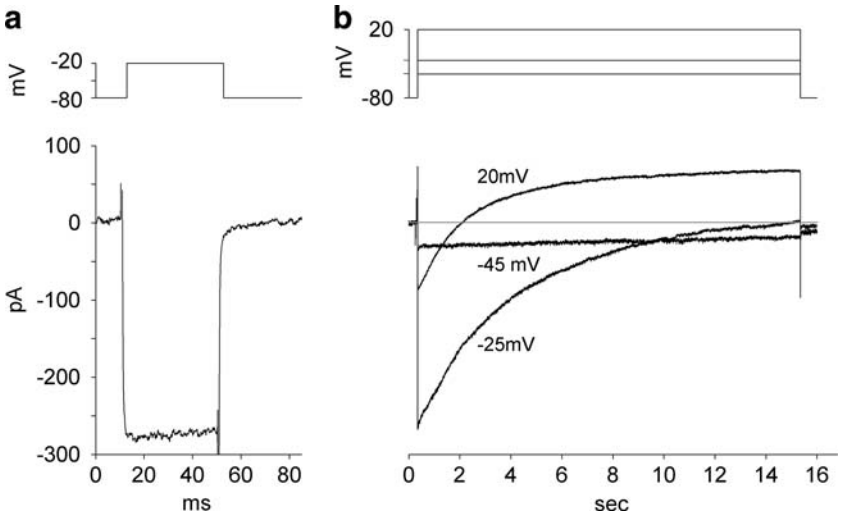

Fig. 4 Current tracings elicited by long depolarisations under control conditions. A cell exhibiting an unusually large Ca^{2+} current (**a**) was subjected to three 15 s steps from −80 mV to −45, −25, and +20 mV (**b**). Despite the initial very large inward current, the current amplitude decayed to 0 and even reversed to outward for the largest depolarisation. Current waveforms very similar to those shown in b were obtained in cells retaining the R1 component, and/or exhibiting smaller Ca^{2+} currents (Fig. 5a), and/or in the presence of 10 mM ATP

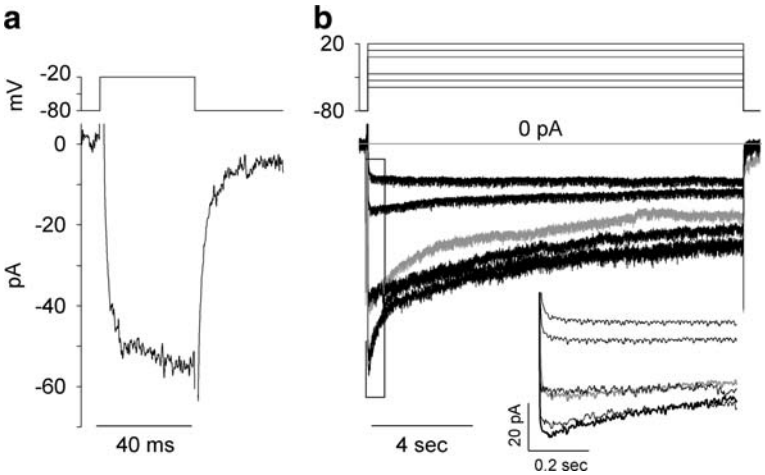

Fig. 5 Representative current family elicited by long depolarisations with internal Cs^+ substituted with NMG^+. Despite the small amplitude (**a**), the current showed a reduced decay and never became outward, even for the largest depolarisation (**b**). For the sake of clarity, the first 0.7 s of the current recordings are enlarged in the inset. In both panels, the grey trace is the current elicited by the depolarisation to 0 mV

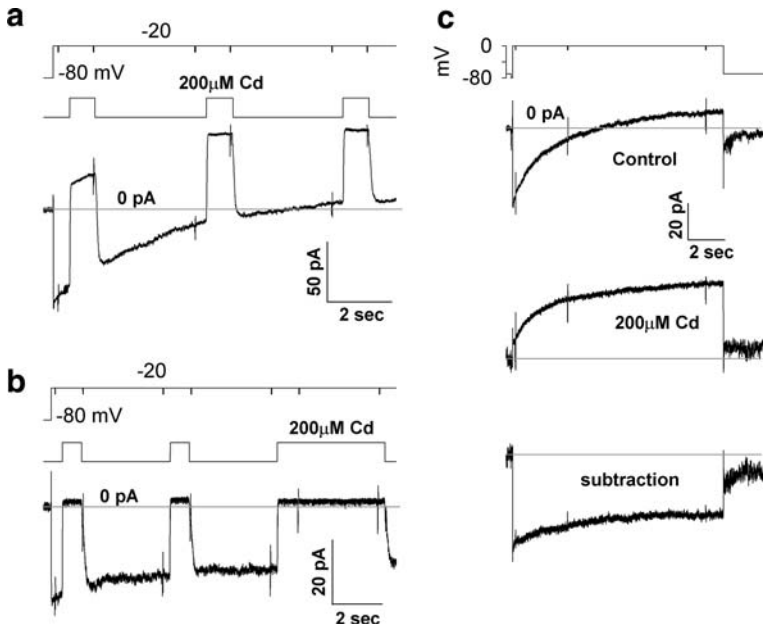

Fig. 6 Ca^{2+} current blockade tested during long-lasting depolarisations. With the cell held at −20 mV, brief 200 μM Cd^{2+} pulses (precise timing is shown below the voltage protocol) were applied at different times under control conditions (**a**) or after internal Cs^{+} was substituted with NMG+ (**b**). **c** The difference between the current waveforms, elicited by a 0 mV voltage pulse under control conditions (*top panel*) and in the presence of 200 μM Cd^{2+} (*middle panel*), isolates the Ca^{2+} current (*lower panel*), which was similar to that shown in Fig. 5b (*grey trace*). Small (−10 mV) and brief (20 ms) voltage pulses were delivered throughout (ticks on current tracings and voltage protocols, here and in Fig. 7) to verify that the membrane resistance remained constant. *Grey straight line* indicates the 0 current level in all panels

larger inward Na^{+} current would be expected upon switching to 100 nM Ca^{2+}; changes in Na^{+} current amplitude, however, were never observed (data not shown). Moreover, the repetitive application of 200 μM Cd^{2+} at increasing times during the current decay reduced the total current by about the same amount (Fig. 6a, b), indicating that the Ca^{2+} current amplitude was little affected throughout the depolarising step. Moreover, the current was almost cancelled by 200 μM Cd^{2+} when internal Cs^{+} was substituted with NMG^{+} (Fig. 6b). The difference tracings recorded at 0 mV under control conditions and in the presence of 200 μM Cd^{2+} provided a current time course with a limited decay (Fig. 6c), very similar to the corresponding trace (grey) shown in Fig. 5b. These findings suggest that Ca^{2+} macrocurrent inactivation was actually very limited when the aspecific outward current component was removed.

External application of 10 μM BayK almost doubled the size of the inward current peak (further confirming that it was entirely carried by Ca^{2+}), without any effect on either the decay time course or amplitude of the outward current (data not shown).

This unexpected behaviour could be sustained by voltage- and/or Ca^{2+}-dependent Cl-channels, slowly activated by the depolarisation. The possibility was explored by using Cl-channel blockers, such as 0.5 mM anthracene-9-carboxylic acid (9AC) or 100 μM niflumic acid, or by altering the Cl^{-} gradient upon partially substituting either the intracellular CsCl with an isoosmolar concentration of Cs-methane-sulfonate, or the extracellular NaCl with Na-isethionate. None of these manoeuvres, however, affected the overall current waveform, that thus did not contain any Cl^{-} ion component.

Finally, the participation of Cs^{+} ions flowing through a non-Ca^{2+} cationic channel, which becomes progressively unblocked during sustained depolarisation, was tested. As expected, a change in the transmembrane Cs^{+} gradient greatly affected the size and waveform of the long-lasting current (Fig. 7a, b). The identity of this cationic channel is still under investigation.

The close relationship between Ca^{2+} current and progressive run-down of the entire current during repeated 5 s depolarisations (Fig. 7c) would suggest that Cs^{+} ions were flowing through Ca^{2+}-activated K^{+} channels, but this hypothesis has been ruled out by experiments using specific K^{+} channel toxins. Alternatively, the Ca-dependent proteases responsible for the Ca^{2+} current run-down (Martini et al. 2000) might be involved in regulating this cationic channel. In either case, maintained depolarisation would eventually unblock the cationic channel, even in the presence of millimolar amounts of Cs^{+} and TEA^{+} in both the internal and the external solutions. In conclusion, the present findings suggest that the selectivity and inactivation mechanism of the channels sustaining the Ca^{2+} macrocurrent in hair cells are stable during long-lasting membrane potential changes.

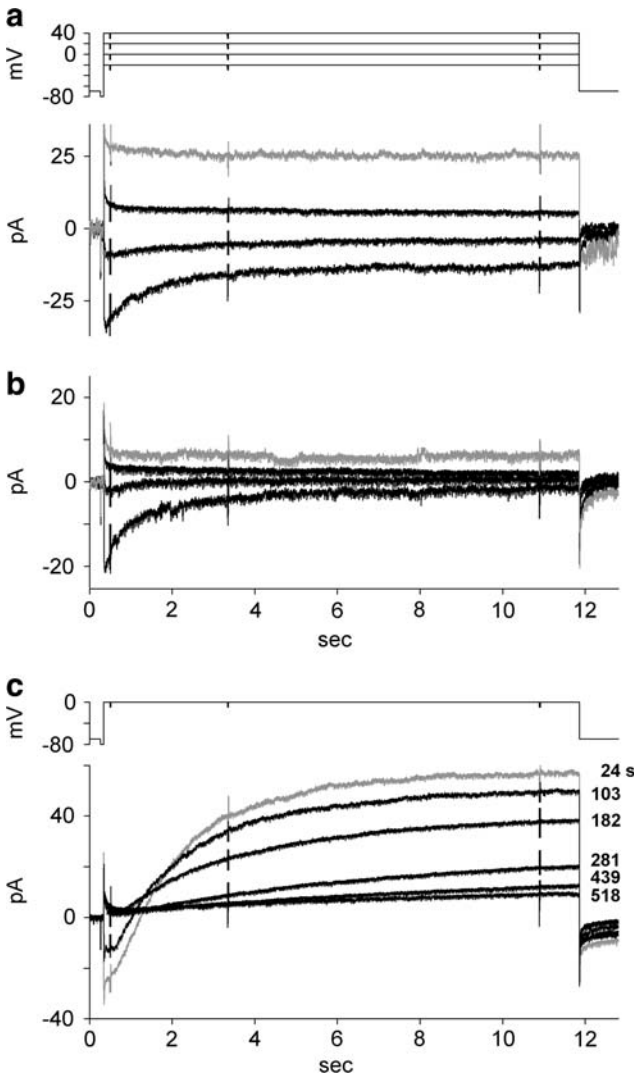

Fig. 7 Outward current properties depend on the Cs^+ gradient. **a** and **b**, responses to long-lasting depolarisation of a hair cell dialysed with 30 mM Cs^+ and extracellularly perfused with 6 mM Cs^+ (**a** Cs^+ equilibrium potential: −40 mV) or 65 mM Cs^+ (**b** Cs^+ equilibrium potential: +20 mV). Note that the inward current fraction is reduced according to the positive shift (**a** vs. **b**) of the Cs^+ equilibrium potential. **c** Run-down of the outward current following repetitive long-lasting voltage steps to 0 mV. Representative traces are shown at selected recording times (indicated close to each trace). For the sake of clarity, the largest outward currents evoked by the depolarisation to +40 mV (**a**, **b**) or by the first depolarisation (**c**) are singled out in *grey*

Acknowledgments The authors are grateful to Dr. Rita Canella for help in some experiments. This work was supported by grants from ASI (contract no.: I/006/06/0), from the Ministero Istruzione Università e Ricerca (MIUR), Rome, and from the "Comitato dei sostenitori dell'Università di Ferrara".

References

Bao H, Wong WH, Goldberg JM, Eatock RA (2003) Voltage-gated calcium channel currents in type I and type II hair cells isolated from the rat crista. J Neurophysiol 90:155–164

Brandt A, Striessnig J, Moser T (2003) Cav1.3 channels are essential for development and presynaptic activity of cochlear inner hair cells. J Neurosci 23:10832–10840

Catterall WA (2000) Structure and regulation of voltage-gated Ca^{2+} channels. Annu Rev Cell Dev Biol 16:521–555

Chen C, Nenov A, Norris CH, Bobbin RP (1995) ATP modulation of L-type calcium channel currents in guinea pig outer hair cells. Hear Res 86:25–33

Dolphin AC (2003) G protein modulation of voltage-gated calcium channels. Pharmacol Rev 55:607–627

Fuchs PA (2002) The synaptic physiology of cochlear hair cells. Audiol Neurootol 7: 40–44

Green GE, Khan KM, Beisel DW, Drescher MJ, Hatfield JS, Drescher DG (1996) Calcium channel subunits in the mouse cochlea. J Neurochem 67:37–45

Hering J, Feltz A, Lambert RC (2004) Slow inactivation of the Ca(V)3.1 isotype of T-type calcium channels. J Physiol 555:331–344

Kollmar R, Montgomery LG, Fak J, Henry LJ, Hudspeth AJ (1997) Predominance of the alpha1D subunit in L-type voltage-gated Ca^{2+} channels of hair cells in the chicken's cochlea. Proc Nat Acad Sci USA 94:14883–14888

Leresche N, Hering J, Lambert RC (2004) Paradoxical potentiation of neuronal T-type Ca^{2+} current by ATP at resting membrane potential. J Neurosci 16:5592–5602

Lelli A, Perin P, Martini M, Ciubotaru CD, Prigioni I, Valli P, Rossi ML, Mammano F (2003) Presynaptic calcium stores modulate afferent release in vestibular hair cells. J Neurosci 23:6894–6903

Lopez I, Ishiyama G, Ishiyama A, Jen JC, Liu F, Baloh RW (1999) Differential subcellular immunolocalization of voltage-gated calcium channel alpha1 subunits in the chinchilla cristae ampullaris. Neuroscience 92:773–782

Martini M, Rossi ML, Rubbini G, Rispoli G (2000) Calcium currents in hair cells isolated from semicircular canals of the frog. Biophys J 78:1240–1254

Martini M, Farinelli F, Rossi ML, Rispoli G (2006) Voltage and ATP regulation of Ca^{2+} channels of vestibular hair cells. Biophys J 90(Suppl 2):237a

Noma A, Shibasaki T (1985) Membrane current through adenosine-triphosphate-regulated potassium channels in guinea pig ventricular cells. J Physiol 363:463–480

O'Rourke B, Backx PH, Marban E (1992) Phosphorylation-independent modulation of L-type calcium channels by magnesium-nucleotide complexes. Science 257:245–248

Platzer J, Engel J, Schrott-Fischer A, Stephan K, Bova S, Chen H, Zeng H, Striessnig J (2000) Congenital deafness and sinoatrial node dysfunction in mice lacking class. D L-type Ca^{2+} channels. Cell 102:89–97

Rodriguez-Contreras A, Yamoah EN (2001) Direct measurement of single-channel Ca^{2+} currents in bullfrog hair cells reveals two distinct channel subtypes. J Physiol 534:669–689

Rodriguez-Contreras A, Nonner W, Yamoah EN (2002) Ca^{2+} transport properties and determinants of anomalous mole fraction effects of single voltage-gated Ca^{2+} channels in hair cells from bullfrog saccule. J Physiol 538:729–745

Rispoli G, Martini M, Rossi ML, Rubbini G, Fesce R (2000) Ca^{2+}-dependent kinetics of hair cell Ca^{2+} currents resolved with the use of cesium BAPTA. Neuroreport 11:2769–2774

Rispoli G, Martini M, Rossi ML, Mammano F (2001) Dynamics of intracellular calcium in hair cells isolated from the semicircular canal of the frog. Cell Calcium 30:131–140

Rossi ML, Martini M, Pelucchi B, Fesce R (1994) Quantal nature of synaptic transmission at the cytoneural junction in the frog labyrinth. J Physiol 478:17–35

Schnee ME, Ricci AJ (2003) Biophysical and pharmacological characterization of voltage-gated calcium currents in turtle auditory hair cells. J Physiol 549:697–717

Su ZL, Jiang SC, Gu R, Yang WP (1995) Two types of calcium channels in bullfrog saccular hair cells. Hear Res 87:62–68

Tucker TR, Fettiplace R (1996) Monitoring calcium in turtle hair cells with a calcium-activated potassium channel. J Physiol 494:613–626

Waka N, Knipper M, Engel J (2003) Localization of the calcium channel subunits Cav1.2 (alpha1C) and Cav2.3 (alpha1E) in the mouse organ of Corti. Histol Histopatol 18:1115–1123

Yazawa K, Kameyama A, Yasui K, Li JM, Kameyama M (1997) ATP regulates cardiac Ca^{2+} channel activity via a mechanism independent of protein phosphorylation. Pflugers Arch 433:557–562